In Vitro Electrochemical Investigations of Advanced Stainless Steels for Applications as Orthopaedic Implants

M. Sivakumar, U. Kamachi Mudali, and S. Rajeswari

Potentiodynamic anodic polarization experiments on advanced stainless steels (SS), such as nitrogen-bearing type 316L and 317L SS, were carried out in Hank's solution (8 g NaCl, 0.14 g $CaCl_2$, 0.4 g KCl, 0.35 g $NaHCO_3$, 1 g glucose, 0.1 g NaH_2PO_4, 0.1 g $MgCl_2$, 0.06 g $Na_2HPO_4 \cdot 2H_2O$, 0.06 g $MgSO_4 \cdot 7H_2O/1000$ mL) in order to assess the pitting and crevice corrosion resistance. The results showed a significant improvement in the pitting and crevice corrosion resistance than the commonly used type 316L stainless steel implant material. The corrosion resistance was higher in austenitic stainless steels containing higher amounts of nitrogen. The pit-protection potential for nitrogen-bearing stainless steels was more noble than the corrosion potential indicating the higher repassivation tendency of actively growing pits in these alloys. The accelerated leaching study conducted for the above alloys showed very little tendency for leaching of metal ions, such as iron, chromium, and nickel, at different impressed potentials. This may be due to the enrichment of nitrogen and molybdenum at the passive film and metal interface, which could have impeded the releasing of metal ions through passive film.

1. Introduction

ORTHOPAEDIC implants are artificial mechanical devices that are mounted to the skeletal system of the human body for various purposes, such as supporting bone, replacing bones or joints, and reattaching tendons or ligaments. These surgical implants are usually made of one of three types of materials: austenitic stainless steels, cobalt-chromium alloys, and titanium and its alloys (Ref 1). Amongst all these materials, titanium and its alloys are most corrosion resistant (Ref 2). However, the main disadvantages are their high cost and special welding procedures required for joining (Ref 3). The austenitic stainless steels, especially type 316L stainless steels, are the most popular ones because of their relative lower costs and reasonable corrosion resistance (Ref 4). However, it was reported that type 316L SS orthopaedic implants corrode in the body environment and release iron, chromium, and nickel ions (Ref 5). These leached chromium and nickel ions are powerful allergens and are carcinogenic in rats (Ref 1). Therefore, high-corrosion resistance is demanded for implants to obtain biocompatibility and acceptability. The failure investigations and survey of failed stainless steel implants removed from human subjects revealed significant localized corrosion attack, for example, pitting (Ref 6, 7) and crevice corrosion (Ref 8, 9), which are the most frequently observed types of corrosion attack. The

above factors necessitated the development of new stainless steel implant materials exhibiting resistance to localized corrosion attack.

In spite of immense strides made in the development of metals for use in orthopaedic surgery, much remains to be improved. Pohler (Ref 10) and Nielsen (Ref 5) suggested adopting the accelerated test in appropriate simulation of human environment for previously untried modified stainless steels to be performed to advantageously replace the currently used type 316L stainless steel.

Nitrogen is considered an important alloying addition to austenitic stainless steel in terms of corrosion resistance. It promotes passivity and widens the passive range in which pitting is less probable (Ref 11-15). So, the previously untried nitrogen-bearing austenitic stainless steel was adopted in this investigation.

The in vitro anodic polarization study is a standard test for the determination of pitting and crevice corrosion resistance of metallic implant materials (Ref 16). However, the polarization study is only a qualitative test to determine the corrosion resistance of the implant alloys (Ref 17). For implants, there is a need for the quantitative determination of corrosion products because of their adverse effects on the human body. An accelerated leaching study by a chronoamperometric method was used to gather quantitative information on the corrosion products (Ref 18). In this method, the corrosion process can be accelerated by impressing an anodic potential in the passive region of the metallic implant material; thus the simulation of a long-time contact between the implant and a normal biological medium is achieved in a reduced time. In the present study, in vitro corrosion behavior was carried out on improved stainless steels, namely nitrogen-bearing austenitic stainless steels, by electrochemical methods. Pitting and crevice corrosion resistance were evaluated, and performance in accelerated leaching under simulated conditions was assessed.

M. Sivakumar and **S. Rajeswari**, Department of Analytical Chemistry, University of Madras, Madras—600 025, India; **U. Kamachi Mudali**, Metallurgy Division, Indira Gandhi Centre for Atomic Research, Kalpakkam—603 102, India.

Table 1 Chemical composition of stainless steels

Alloy	Composition, wt%								
	Cr	Ni	Mo	Mn	P	S	Si	N	C
316L	17.2	12.7	2.1	2.05	0.017	0.003	0.521	...	0.021
316LN1	17.9	12.2	2.45	2.11	0.025	0.002	0.975	0.068	0.025
316LN2	17.4	13.2	2.57	1.91	0.021	0.003	0.640	0.160	0.019
317LN1	18.22	13.3	3.04	2.21	0.025	0.002	0.30	0.088	0.022
317LN2	18.47	14.18	3.58	1.92	0.032	0.001	0.69	0.141	0.014

2. Materials and Methods

2.1 Electrode Preparation

The five alloys used in this investigation are: 316L stainless steel (316L); 316L, 680 ppm of nitrogen (316LN1); 316L, 1600 ppm of nitrogen (316LN2); 317L, 880 ppm of nitrogen (317LN1); and 317L, 1410 ppm of nitrogen (317LN2).

Elemental compositions of the above alloys are given in Table 1. Alloys were cut into 1 cm × 1 cm × 0.5 cm size specimens, annealed for 1 h at 1323 K, and water quenched. Specimens were soldered to a copper rod to provide electrical contact. They were then doped with epoxy resin in such a way that one of its sides with 1 cm² surface area alone was exposed out; this formed the working electrode. In order to avoid severe polishing after the resin mounting (which might cause microcracking at the metal-resin interface), the specimens were wet ground with SiC papers down to 600 grit followed by 5 and 1 μm diamond paste before mounting. The edges of the mounted specimens were examined at 100× (oil immersion) objective lens in an optical microscope for the appearance of any gap between the metal and epoxy resin. If any gap was seen, the specimens were remounted. Then the electrodes were ultrasonically cleaned for 3 minutes and passivated in a solution of 30% HNO₃ (V/V) at 60 °C for 30 minutes, thoroughly washed in deionized water, rinsed in alcohol, and dried.

2.2 Polarization Cell Assembly

A three compartment electrochemical cell (borosilicate glass) with a capacity of 500 mL was adopted. A platinum foil was used as the counter electrode, and a saturated calomel electrode (SCE) was used as the reference electrode. The electrolyte used was a Hank's solution (composition shown in Table 2), and its pH was adjusted to 7.00 ± 0.05 with sodium bicarbonate and maintained at 37 ± 1 °C by a water bath. The test solution was continuously purged with nitrogen. Then the working electrode was introduced into the cell, and the potential was allowed to stabilize for 20 minutes.

2.3 Pitting Corrosion

In the anodic polarization study, the potential was increased in the noble direction at a rate of 0.166 mV/s until the breakdown potential (E_b) was attained where the alloy entered the transpassive or pitting region. The sweep direction was reversed after reaching an anodic current density of 0.5 mA/cm² until the reverse scan reaches the passive region. The potential at which the reverse anodic scan meets the passive region is the pit-protection potential (E_p).

Table 2 Composition of artificial physiological solution (Hank's balanced salt solution)

Compound	Concentration, g/L
NaCl	8.00
CaCl₂	0.14
KCl	0.40
NaHCO₃	0.35
Glucose	1.00
NaH₂PO₄	0.10
MgCl₂ · 6H₂O	0.10
Na₂HPO₄ · 2H₂O	0.06
MgSO₄ · 7H₂O	0.06

After each of the above experiments, the specimens were observed in an optical microscope to investigate the morphology of attack. In pitting corrosion experiments, the pits were allowed to grow up to a current density of 10 mA/cm² for all the specimens. After removing from the electrochemical cell, these specimens were thoroughly washed in distilled water, ultrasonically cleaned in acetone, and dried before observing in the microscope. An MeF-2 Reichert optical metallurgical microscope, Schott Fiber Optics, Southbridge, Massachusetts, was used in the present study.

The parameters of interest that were recorded during cyclic potentiodynamic polarization tests were: the corrosion potential, E_{corr}; the pitting potential, E_b; the pit protection potential, E_p; and the safe region to corrosion attack, ΔE. They are illustrated schematically in Fig. 1.

2.4 Crevice Corrosion

A glass assembly was designed as described by Dayal et al. (Ref 19) to create a crevice on the mounted electrodes. The tip of the glass rod was brought into close contact with the electrode surface using the nut and threaded rod arrangements. The angle between the glass and the electrode surface was maintained at 1.2° ± 0.2°, and the bulk crevice area ratio was 5.6 ± 1.5:1.

To rule out any possibility of pitting and edge attack on electrode surface soon after the experiment, the electrode surface was thoroughly examined in an optical microscope. The electrodes with edge attack were rejected. Those electrodes without edge attack were considered for the study.

2.5 Accelerated Leaching

In the accelerated ageing study, working electrodes were immersed in Hank's solution and allowed to stabilize at constant potentials of +200 mV, +300 mV, +500 mV, and E_b for one
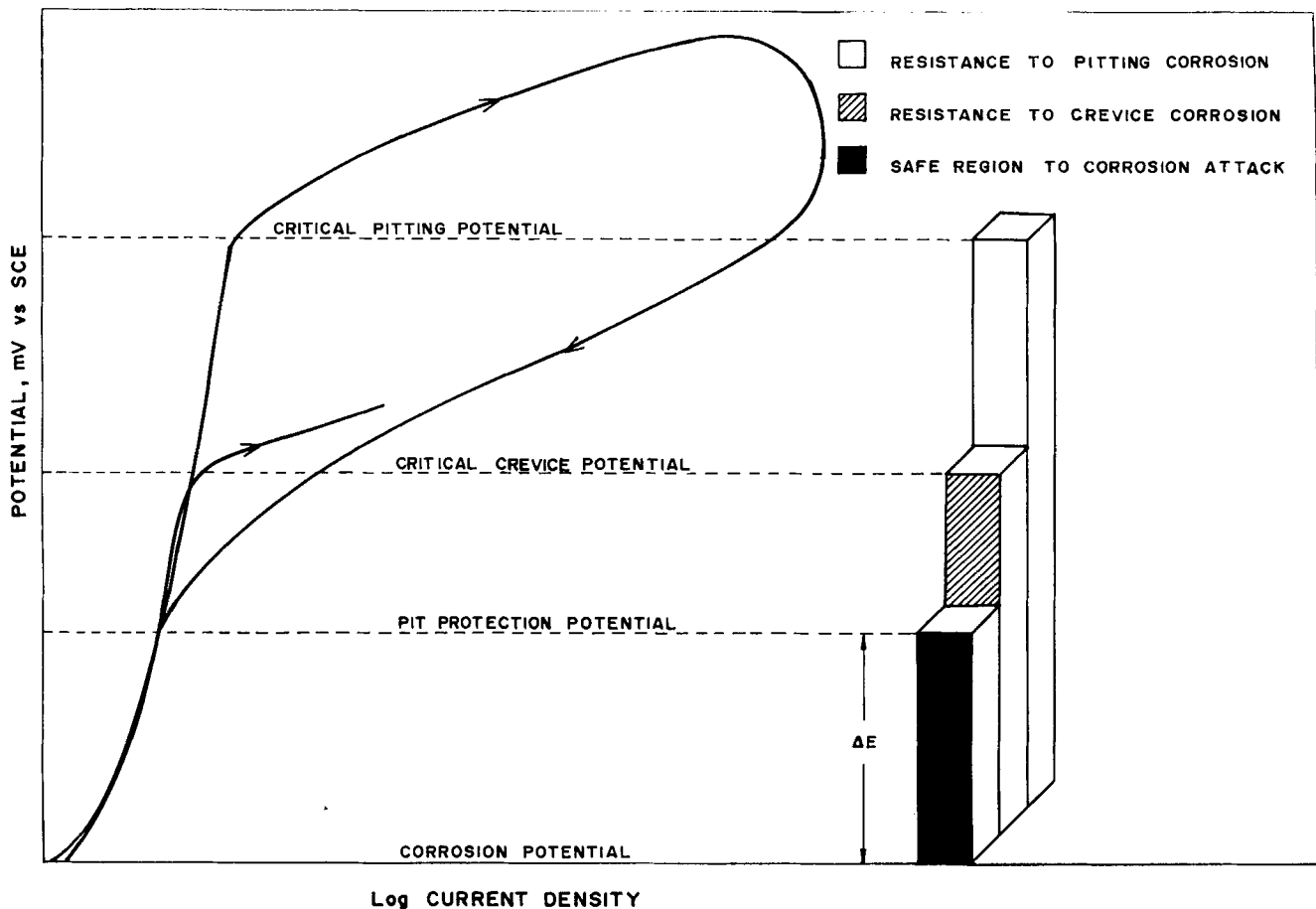
Fig. 1 Potentiodynamic anodic polarization curves for austenitic stainless steels with and without the presence of crevice. Bar diagram indicates the pitting, crevice, and pit-protection behaviors observed from the polarization curves.

hour in 100 mL of solution. At the end of each experiment, the chemical composition of the test solution was analyzed by an inductively coupled plasma-atomic emission spectrometry, and the data were compared with the compositions of the steels listed in Table 1.

3. Results and Discussion

3.1 *Critical Pitting Potential*

The critical pitting potential for 316L, 316LN1, 316LN2, 317LN1, and 317LN2 were determined from the polarization curves. They are shown in Fig. 2. The mean value of critical pitting potential, E_b, for type 316L stainless steel was +365 mV. The presence of 680 ppm of nitrogen in this stainless steel increased the E_b value to +620 mV whereas the presence of 1600 ppm of nitrogen increased the E_b value to +1179 mV. A similar influence of nitrogen was also found in type 317L stainless steel containing 880 ppm and 1410 ppm of nitrogen (see Table 3). Evidently, the austenitic stainless steel with higher nitrogen content exhibited increased E_b value. They improved the pitting corrosion resistance under simulated body conditions.

Morphology of the pitting attack on the above stainless steels is shown in Fig. 3. Type 316L SS exhibits individually smaller (roughly hemispherical) and deeper pits over the entire surface area of the specimen as shown in Fig. 3(a). This indicates higher susceptibility of the material towards pitting attack.

The increase of nitrogen content to 680 ppm in 316L SS revealed a lesser number of pits on those surfaces than the reference 316L SS. The geometry of pits observed were individually larger when compared with type 316L SS. The enhanced pitting potential provided high activation energy for the dissolution of alloy with the pit and accounted for the larger area. An almost identical pitting behavior was observed with 317L SS containing 880 ppm of nitrogen (Fig. 3c).

Further increase in nitrogen content of the 317L SS to 1410 ppm revealed very few pits. However, geometry of the pits observed was larger, shallower, and slightly saucer shaped with smaller depth as shown in Fig. 3(d). Type 316L SS with 1600 ppm of nitrogen still showed a reduced number of pits on the surface. The geometry of the pits was almost identical to that of 317L SS with 1400 ppm of nitrogen (Fig. 3e).

From the optical microscopic observation, the materials with higher corrosion resistance exhibit the lowest depth of at-

Table 3 Electrochemical parameters of polarization curves

Material	E_{corr}, mV	E_{pit}, mV	E_{prot}, mV	E, mV	E_{cc}, mV
316L	−108	365	24	132	272
316LN1 (680)	−168	620	93	261	459
316LN2 (1600)	−159	1179	137	296	730
317LN1 (880)	−145	720	120	265	580
317LN2 (1410)	−155	1152	134	289	756

Note: E_{corr} is corrosion potential. E_{pit} is pitting potential. E_{prot} is pit-protection potential. ΔE is relative corrosion resistance. E_{cc} is critical crevice potential.
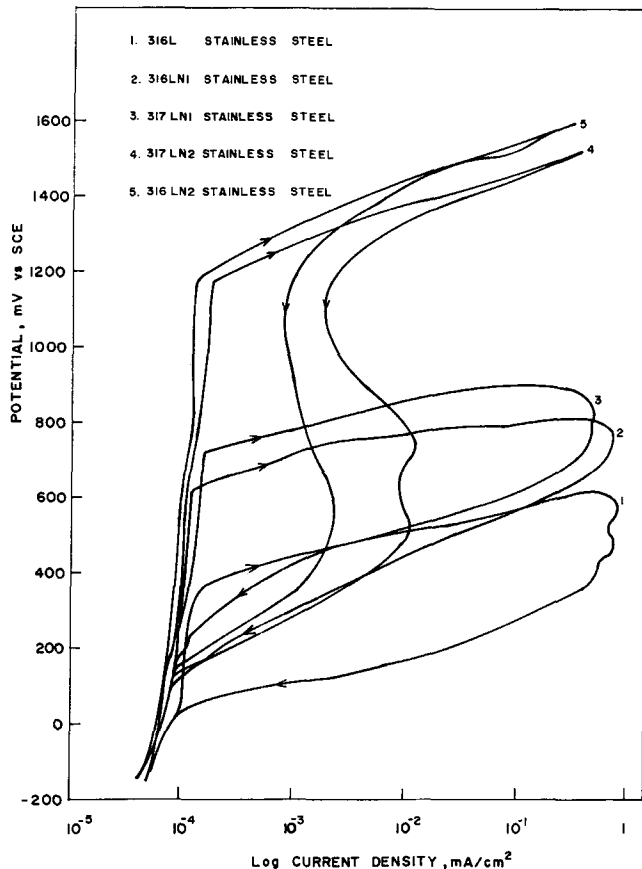
Fig. 2 Potentiodynamic anodic polarization curves for type 316L and nitrogen-bearing austenitic stainless steels

tack, whereas those materials with lesser corrosion resistance revealed the greatest depth of attack. This could be due to the smaller and deeper pits present in the low-ranked alloys where the pH within the pits is very low and aggressive. Therefore, the propagation of pits will be accelerated. In contrast, the larger pits are exposed to the bulk environment. Therefore, the pH within the pits will be increased to solution pH. As a result, the aggressiveness of the environment within pits is reduced.

Type 316L stainless steel contained molybdenum in the range of 2 to 3 wt% whereas 317L stainless steel contained 3 to 4 wt%. The presence of molybdenum inhibits the corrosion process by the formation of a molybdenum salt film, which apparently increased the difficulty in breaking down the passive film (Ref 20).

The present study showed an increased value of the critical pitting potential for nitrogen-bearing austenitic stainless steels; that was significant in the presence of molybdenum. A synergistic influence of nitrogen and molybdenum on the pitting corrosion resistance was reported by Truman et al. (Ref 21) and Newman et al (Ref 22). Clayton (Ref 23) noticed an enrichment of molybdenum and nitrogen at the passive film and metal interface. They attributed this enrichment of nitrogen and molybdenum interface to prevent the further dissolution of the substrate followed by the destruction of the passive film. Kamachi Mudali et al. (Ref 24, 25, 26) reported that the addition of nitrogen improved the pitting resistance and reported a nitrogen equivalent of molybdenum as 530 ppm per weight percentage of molybdenum for the austenitic weld metals.

The bar diagram in Fig. 4 depicts the electrochemical behaviors, namely critical pitting potential, pit-protection potential, and critical crevice potential of nitrogen-bearing austenitic stainless steel in simulated conditions in which the entire bar height in each case represents the pitting resistance. The presence of 680 ppm of nitrogen in 316L stainless steel showed an increase of 70%, and the presence of 1600 ppm of nitrogen exhibited an increase of 220% in the pitting corrosion resistance. Similar influence of nitrogen was observed in type 317L SS with 880 ppm (97%) and 1400 ppm (215%) of nitrogen (see Table 3). From the foregoing observations, the alloys are ranked in the increasing order of pitting corrosion resistance as: 316L < 316LN1 < 317LN1 < 317LN2 < 316LN2.

3.2 Pit-Protection Potential

The pit-protection potential was determined for the above alloys from the polarization curves (Fig. 2). The mean value of pit-protection potential for type 316L stainless steel increased from +24 mV to +93 mV for the presence of 680 ppm of nitrogen whereas the value increased from +24 mV to +137 mV for the presence of 1600 ppm of nitrogen. A similar trend was found for type 317L stainless steel containing 880 and 1410 ppm of nitrogen. The significance of these observations is that new pits cannot be initiated above this potential. Hence, the increased nitrogen content hinders the development of new pits and slows down the kinetic of actively growing pits.

The significant role of nitrogen in the pit-protection potential can be explained by the following facts. Once the passive film is damaged, the formation of pit commences on the metal surface. If the pit grows, the conditions prevailing at that pit site will be similar to that of the active dissolution stage. In general during active dissolution, the alloying elements, such as iron, chromium, and nickel, dissolve whereas nonactive elements,
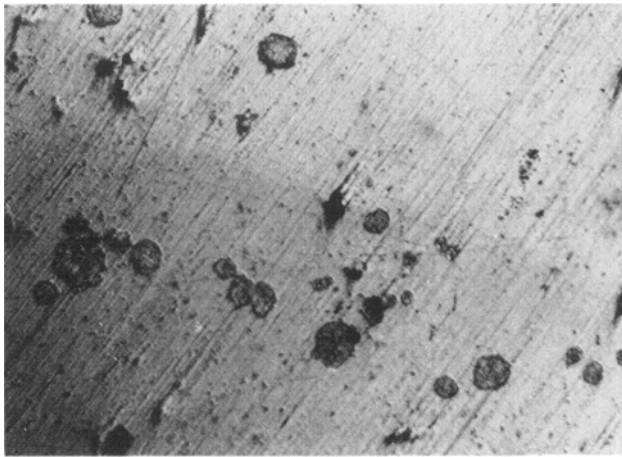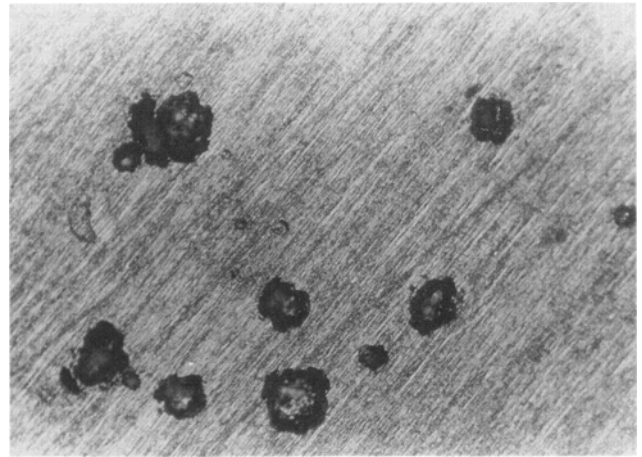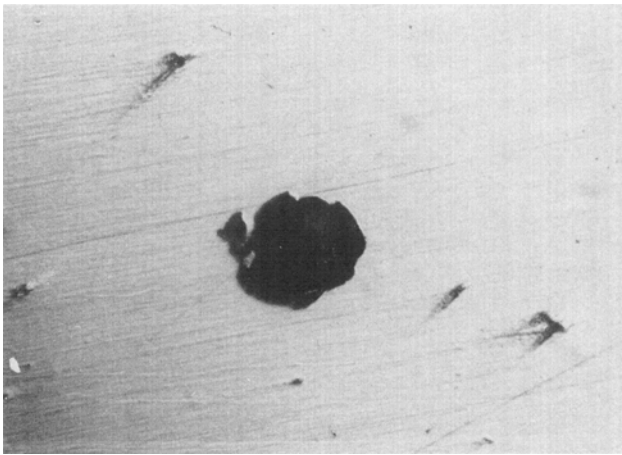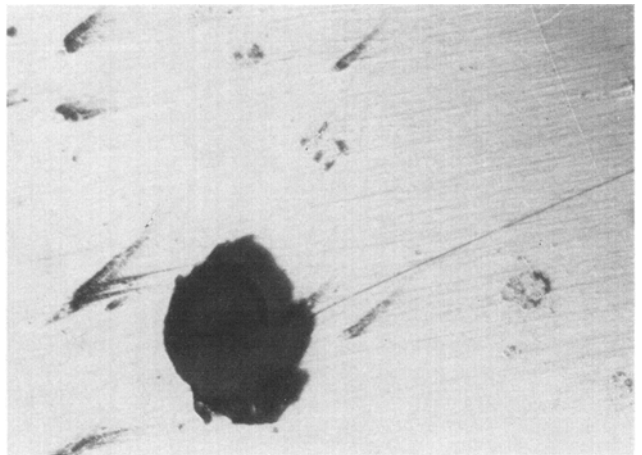
Fig. 3 Pit morphologies of nitrogen-bearing stainless steels in the simulated body conditions. (a) 316L SS. (b) 316L SS with 680 ppm of nitrogen. (c) 317L SS with 880 ppm of nitrogen. (d) 317L SS with 1410 ppm of nitrogen and 316L SS with 1600 ppm of nitrogen
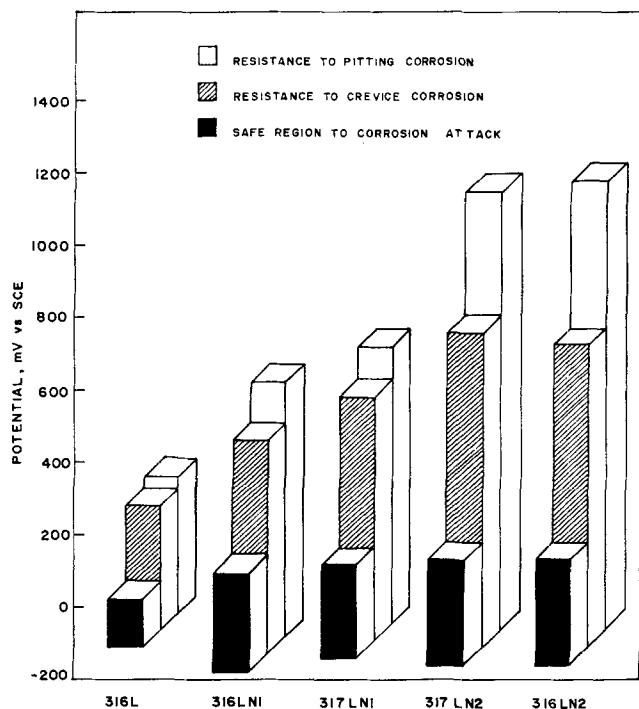
Fig. 4 Bar diagram represents the pitting, crevice, and pit-protection behavior of type 316L and nitrogen-bearing austenitic stainless steels observed from the polarization curves
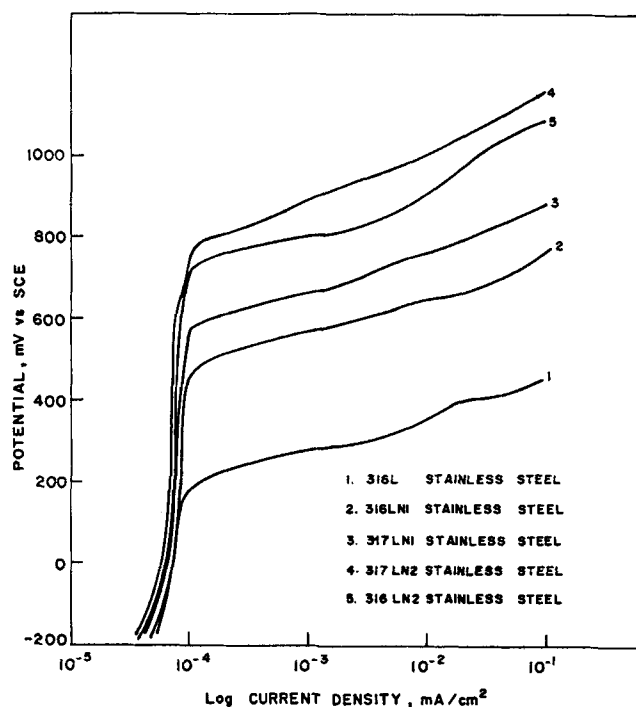

Fig. 5 Potentiodynamic anodic polarization curves for type 316L and nitrogen-bearing austenitic stainless steels in the presence of a crevice

such as nitrogen, can enrich at such surface. Such a segregation was reported by Newman et al. (Ref 22) and by Clayton and Martin (Ref 27) at least to the level of seven times the original concentration of nitrogen present in the alloy. This stage leads to the formation of ammonium ions and subsequently nitrogen compounds, or it may provide an inactive layer to improve the pitting corrosion resistance.

The difference between the pit-protection potential and the corrosion potential for a given system is defined as the relative corrosion resistance, ΔE. This value can be used to rank the alloys. The mean value of E for 316L stainless steel was 132 mV. The presence of 680 ppm of nitrogen in this stainless steel increased the ΔE value to 261 mV whereas the presence of 1600 ppm of nitrogen increased the ΔE value to 296 mV. A higher value of ΔE reflects an enhanced resistance to pitting or accelerated general corrosion. The presence of 880 ppm and 1410 ppm of nitrogen in 317L stainless steel also showed similar increase in E value as shown in Table 3. This study indicated a beneficial influence of nitrogen to austenitic stainless steels.
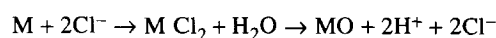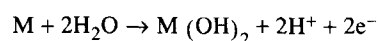
The dark portion in the bar diagram (Fig. 4) represents the safe region to corrosion attack. It clearly indicates the beneficial effect of nitrogen for both 316L and 317L stainless steels.

3.3 Critical Crevice Potential

Crevice corrosion (corrosion between the screws and plate or other contacting areas) occurs in almost all multicomponent 316L stainless steel orthopaedic devices. This type of corrosion can cause sufficient clinical reaction to necessitate the removal of the implant (Ref 9). Crevice corrosion of the implant can be determined by the anodic polarization method.

The critical crevice potential, E_{cc}, was determined from the polarization curves of the materials studied by the anodic polarization method. They are shown in Fig. 5. The presence of 680 ppm nitrogen in 316L stainless steel increased the E_{cc} value to +459 mV from +272 mV, and the presence of 1600 ppm of nitrogen raised the E_{cc} value to +730 mV. Similar influence of nitrogen addition was found for type 317L stainless steel containing 880 and 1410 ppm of nitrogen with respect to the critical crevice potential (Table 3). Thus the present study showed the beneficial effect of nitrogen addition in improving the crevice corrosion resistance of austenitic stainless steels.

The pH of the normal body fluid is 7.4. In this condition, oxygen is the principal depolarizer; oxygen present at the implant crevice is consumed quite rapidly either in the cathodic reaction or for passivation. This inhomogeneity in oxygen concentration leads to the formation of a concentration cell. However, the change in the pH of the medium seems to be of greater importance than the change in the oxygen concentration (Ref 28). Acidification of the crevice area can take place as a result of anodic reaction.

$$M + H_2O \rightarrow MO + 2H^+ + 2e^-$$

$$M + 2H_2O \rightarrow M\,(OH)_2 + 2H^+ + 2e^-$$

$$M + 2Cl^- \rightarrow M\,Cl_2 + H_2O \rightarrow MO + 2H^+ + 2Cl^-$$

The acidification can accelerate the anodic reaction in the crevices (Ref 28). The addition of nitrogen to austenitic stainless steels improved the crevice corrosion resistance due to the
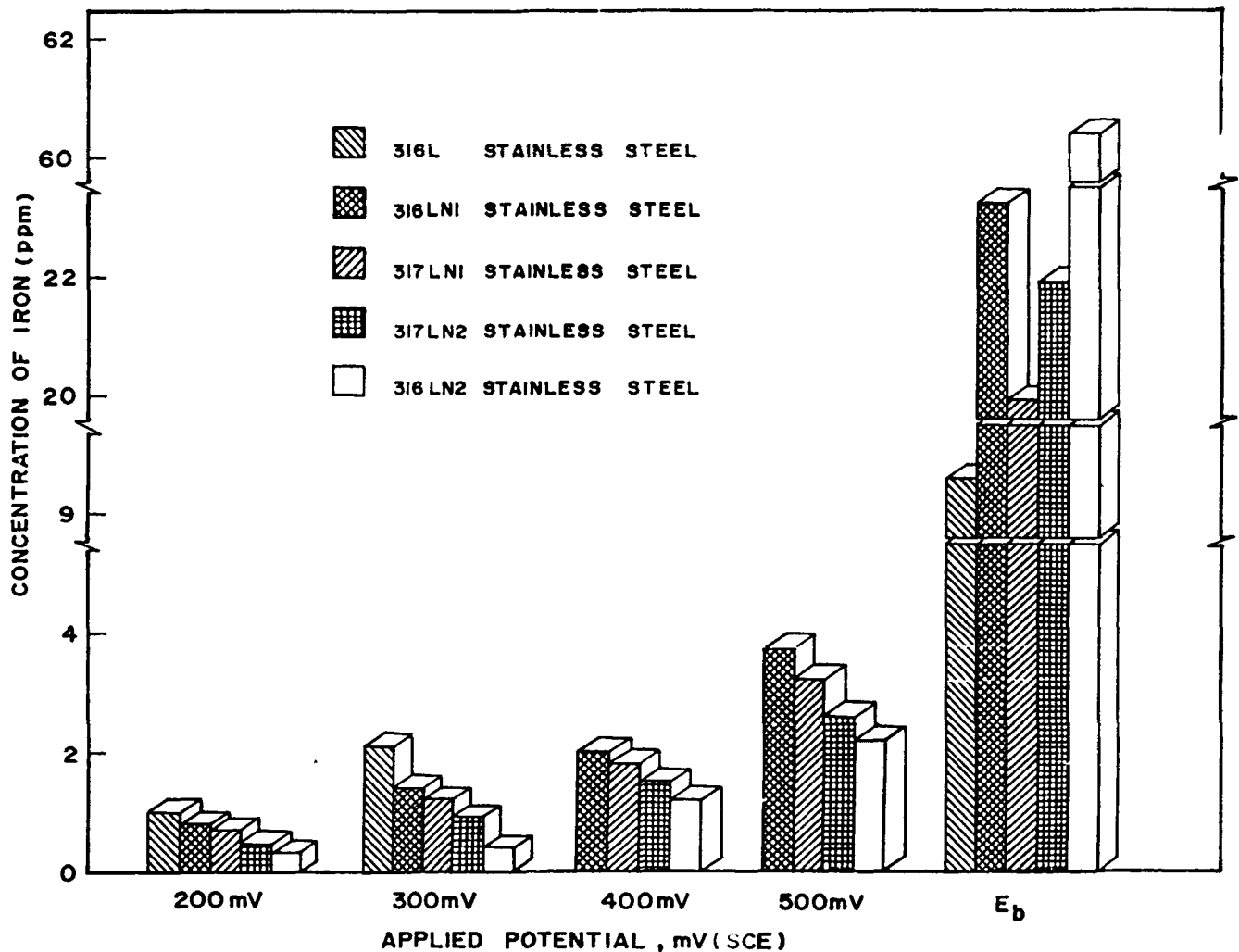
Fig. 6 Concentration of iron present in the solution after accelerated leaching of stainless steels at different impressed electrode potentials

formation of ammonium ions at the pits present in the crevices, which increased the pH and slowed down the pit growth kinetics. Clayton (Ref 23) suggested a chemical rather than an electrochemical mechanism for the formation of ammonium ions, and pH was controlled by the formation of nitrides formed from the anodically segregated nitrogen. Kamachi Mudali et al. (Ref 24) showed the dissolution of nitrogen at the pit site and subsequent formation of ammonium ions and nitrate compounds, which improved the pitting corrosion resistance:

$$N + 4H^+ + 3e^- \rightarrow NH_4^+$$
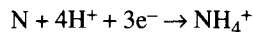
Thus the effect of localized decrease in pH at the crevice area can be avoided by using nitrogen-bearing austenitic stainless steel as implant material.

The nitrogen-bearing stainless steels showed a similar trend of pitting and crevice corrosion resistance. The results of this investigation indicate that the pitting corrosion resistance and the crevice corrosion resistance are interrelated and that an im-

provement in the pitting corrosion resistance is generally accompanied by an improvement in the crevice corrosion resistance. However, 317LN2 showed a higher crevice corrosion resistance than 316LN2. This increased corrosion resistance is due to the fact that 317LN2 contains higher Ni content than 316LN2 stainless steel (Table 1). The presence of higher nickel content raises the critical crevice potential in the noble direction, thereby rendering the breakdown of passive film within the crevice more difficult.

In addition, the hydrolysis of Ni^{2+} yields essentially a neutral pH so that the dissolved nickel ions are not likely to contribute to the acidification of the solution within the crevice. In a similar manner, the beneficial effect of increasing the chromium content can probably be attributed to the fact that chromium also raises the pitting potential in the noble direction, rendering the film breakdown within the crevice more difficult. However, unlike nickel ions, chromium ions hydrolyze to yield a very low pH. It will accelerate the corrosion process, and therefore, chromium may not provide adequate crevice corrosion resistance.
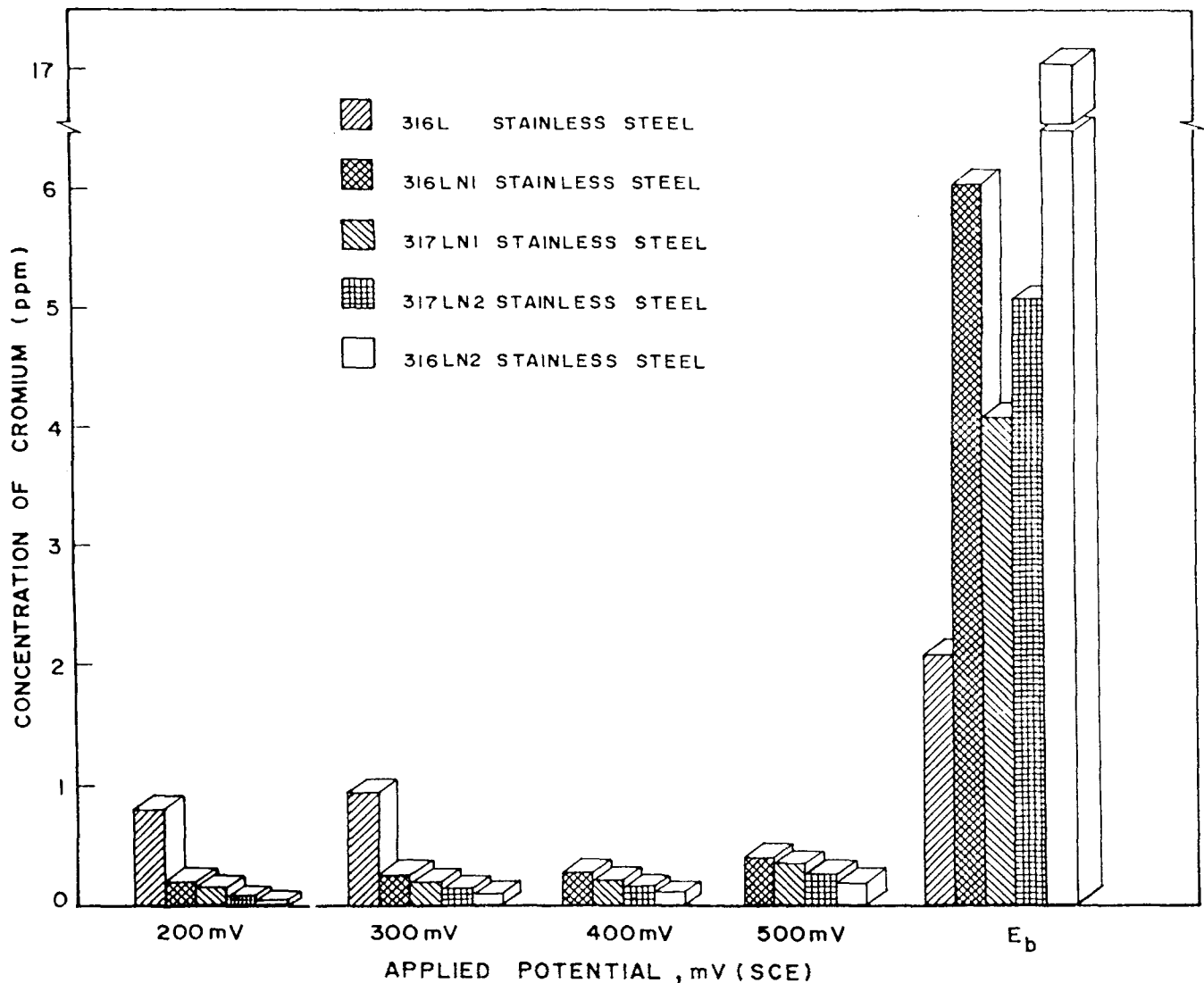
Fig. 7 Concentration of chromium present in the solution after accelerated leaching of stainless steels at different impressed electrode potentials

Crevice corrosion resistance was determined for the nitrogen-bearing stainless steels and is plotted in the form of a bar diagram (Fig. 4). The shaded portion in each case represents the resistance to crevice corrosion. The extent of resistance to crevice corrosion increased with increase in nitrogen alloying in austenitic stainless steels. The increasing order of crevice corrosion resistance was: 316L < 316LN1 < 317LN1 < 316LN2 < 317LN2.

3.4 Accelerated Leaching in Simulated Body Conditions

In the accelerated leaching study, the concentration of metal ions, i.e., iron, nickel, and chromium, present in the test solution after ageing for one hour was determined; the results are illustrated in Fig. 6, 7, and 8. A significant amount of metal ions was released into the solution even in the passive region of 316L stainless steel implant material.

At an impressed potential of 200 mV, the increasing order of leaching of the metal ions into the test solution was 316LN2 < 317LN2 < 317LN1 < 316LN1 < 316L. A similar trend of leaching of metal ions was observed at other impressed potentials at +300, +400, and +500 mV.

Type 316L stainless steel was subjected to the pitting attack at +365 mV; hence, the leaching study was not conducted at +400 mV and +500 mV.

In in vivo conditions, the released metal ions from the implants are transported to the remote tissues through body fluids. They induce cytotoxic and allergic reactions and cause cancer (Ref 1). This study indicated that nitrogen-bearing stainless steels showed very low leaching of metal ions at the potentials impressed in the passive region. This may be due to the enrichment of nitrogen at the passive film and metal interface, which could have impeded the releasing of metal ions through passive film by strengthening the interface (Ref 22). Nitrogen present
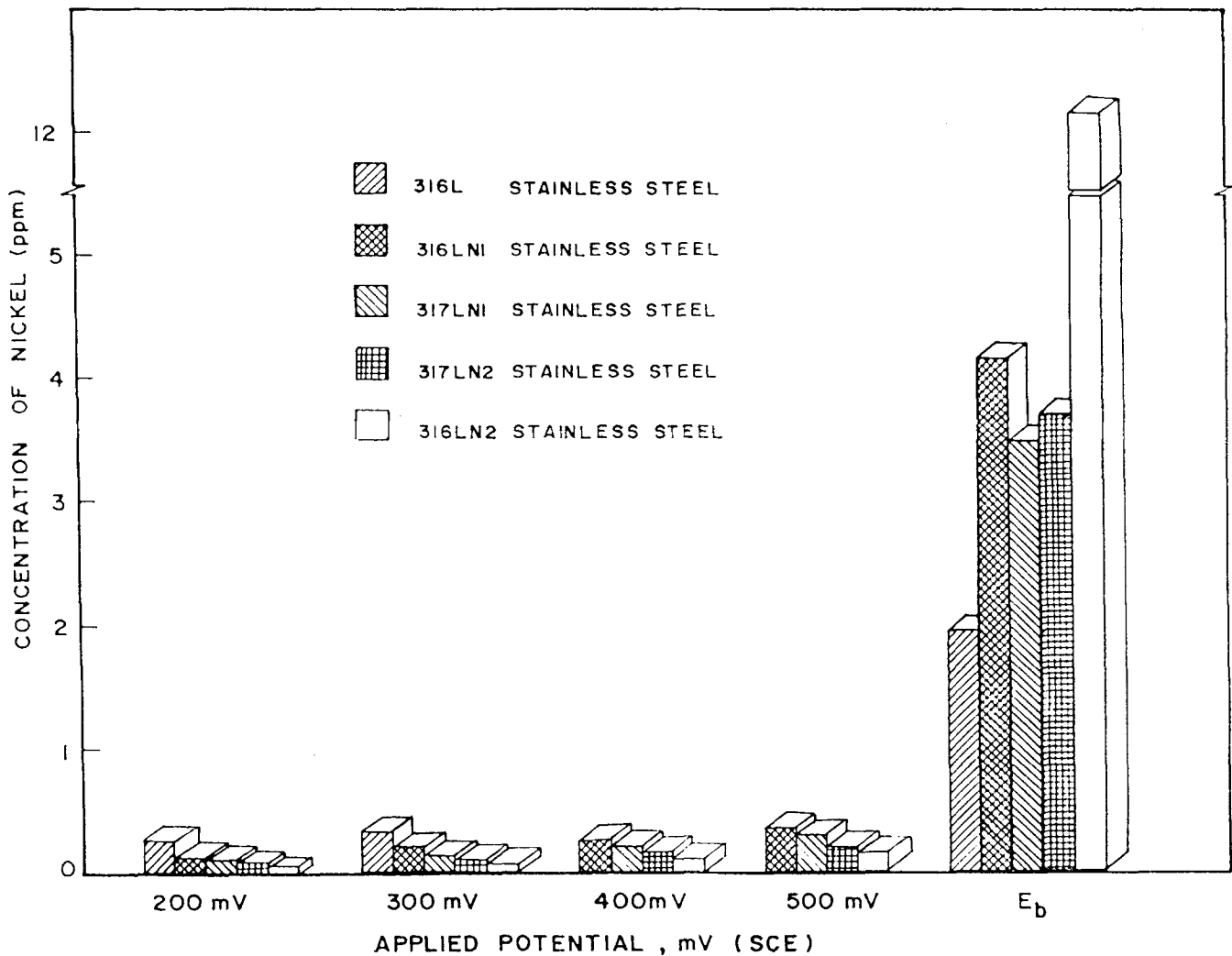
Fig. 8 Concentration of nickel present in the solution after accelerated leaching of stainless steels at different impressed electrode potentials

in the alloy reversibly impedes active dissolution over a small range of potential. This may indicate the occurrence of a crossover of the rates of metal dissolution (anodic) and nitrogen dissolution (cathodic) leading to an enrichment of nitrogen atoms on the monoatomic surface (Ref 29).

At the pitting potential, the increasing order of leaching of the metal ions was 316L < 317LN1 < 317LN2 < 316LN1 < 316LN2. Nitrogen-bearing stainless steels showed enhanced leaching of the metal ions iron, nickel, and chromium at the pitting potential. This can be related to the potential at which pitting occurs in the above alloys. Nitrogen improves the passive film, and a higher potential is required to initiate pitting compared to the low nitrogen alloy. Therefore, the high potential at which pitting occurs may cause the pit to grow faster, so the release of metal ions was high in the nitrogen-bearing stainless steel at the pitting potential.

At the pitting potential, alloys 317LN1 and 317LN2 showed a lesser dissolution of metal ions than alloys 316LN1 and 316LN2 in the present study. Alloys 316LN1 and 317LN2 con-

tain 10,000 and 12,000 ppm of molybdenum higher than that of alloys 316LN1 and 316LN2. It was reported that segregation of molybdenum and nitrogen at the passive film and substrate interface occurs during passive film formation (Ref 22). This enrichment could have impeded the further dissolution of iron, chromium, and nickel in alloys 317LN1 and 317LN2 at the pitting potential compared to alloys 316LN1 and 316LN2. The accelerated leaching study results compliment the pitting and crevice study observations.

3.5 Environment of Implanted Material in Fractured Bone Site

Though normal body fluids are neutral pH (7.4), an acidic condition was reported at the implanted site of the bone fracture (Ref 30). The pH in the early periods following surgery drops to 4, and in the course of only 10 to 15 days, the pH attains neutrality. If wound healing is delayed, a lower pH will persist (Ref 30). The decrease in pH at such critical sites will induce pitting corrosion (Ref 6). Normally the implant placed on the fractured

bone is subjected to the unbalanced weight-bearing biomechanical forces resulting in bending and torsional stresses, and the implant may undergo a cyclic loading (Ref 10). The propagation of stress corrosion and corrosion fatigue cracks and mechanical fatigue fracture can originate from the corrosion pits (Ref 6, 7). The effect of local decrease in pH on the stainless steel implant at the fractured bone site can be avoided by using nitrogen-bearing austenitic stainless steels as implant material because the nitrogen released from these alloys at such critical sites can form ammonium ions by utilizing H^+ ions.

4. Conclusions

The present investigation shows:

- Pitting and pit-protection potentials of nitrogen-bearing austenitic stainless steels were nobler than those of presently used 316L stainless steel. The higher pitting and pit-protection potentials indicated the beneficial effect of nitrogen in improving the pitting resistance of austenitic stainless steels. The repassivation of actively growing pits is considerably increased in these alloys.
- Nitrogen-bearing stainless steels showed superior resistance to crevice corrosion than 316L stainless steel. Nitrogen present in this alloy is attributed to ammonium ions and ammonium nitrides at the pits present in the crevices, which slowed down pit growth kinetics because of the increase in pH of the solution inside the pits.
- The accelerated leaching study indicated that releasing of iron, chromium, and nickel from the nitrogen-bearing austenitic stainless steels was considerably less compared to type 316L stainless steel.
- The localized corrosion resistance of 316LN2 (17.4% Cr, 13.2% Ni, 2.57% Mo, 0.16% N, and 0.019% C) and 317LN2 (18.47% Cr, 14.18% Ni, 3.58% Mo, 0.141% N, and 0.014% C) alloys in the simulated body environment were sufficiently higher to prevent the onset of pitting corrosion and crevice corrosion.

Acknowledgments

References

1. D.F. Williams, *J. Mater. Sci.*, Vol 22, 1987, p 3421
2. N. Bruneel and J.A. Helsen, *J. Biomed. Mater. Res.*, Vol 22, 1988, p 203
3. L.H. Boulton and A.J. Betts, *Br. Corros. J.*, Vol 26 (No. 4), 1991, p 287
4. Tzyy-Ping Cheng, Wen-Ta Tsai, and Ju-Tung Lee, *J. Mater. Sci.*, Vol 25, 1990, p 936
5. K. Nielsen, *Br. Corros. J.*, Vol 22 (No. 4), 1987, p 272
6. M. Sivakumar and S. Rajeswari, *J. Mater. Sci. Lett.*, Vol 11, 1992, p 1039
7. M. Sivakumar, U. Kamachi Mudali, and S. Rajeswari, *J. Mater. Sci.*, (in press)
8. D.L. Levine, *J. Biomed. Mater. Res.*, Vol 11, 1977, p 553
9. S.G. Steinemann, Corrosion of Surgical Implants—In vivo and In vitro Tests, *Evaluation of Biomaterials*, G.D. Winter et al., Ed., John Wiley & Sons, 1980, p 1
10. O.E.M. Pohler, *Failure Analysis and Prevention, Metals Handbook*, Vol 11, American Society for Metals, 9th ed., 1986, p 670
11. J.J. Eckenrod and C.W. Kovach, *Properties of Austenitic Stainless Steels and Their Weld Metals (Influence of Slight Chemistry Variations)*, ASTM STP 679, American Society for Testing and Materials, 1979, p 17
12. J.R. Kearns, *J. Mater. Eng.*, Vol 7, 1985, p 16
13. J.E. Truman, *Proceedings of International Conference on High Nitrogen Steels HNS 88*, J. Foct and A. Hendry, Ed., The Institute of Metals, Lille, France, 1989, p 225
14. T. Ogawa, S. Aoki, T. Sakamoto, and T. Zaizen, *Weld. J.*, Vol 61, 1982, p 139
15. T.A. Mozhi, K. Nishimoto, B.E. Wilde, and W.A.T. Clark, *Corrosion*, Vol 42, 1986, p 197
16. K. Merritt and S.A. Brown, *J. Biomed. Mater. Res.*, Vol 22, 1988, p 111
17. H.J. Mueller and E.H. Greener, *J. Biomed. Mater. Res.*, Vol 4, 1970, p 20
18. J.P. Bellier, J. Lacoeur, C. Koehler, and J.P. Davidas, *Biomaterials*, Vol 11, 1990, p 55
19. R.K. Dayal, N. Parvathavarthini, and J.B. Gnanamoorthy, *Br. Corros. J.*, Vol 18 (No. 4), 1983, p 184
20. Wu Yang, Rul-chng Hua and Hul-zhong Hua, *Corros. Sci.*, Vol 24, 1984, p 691
21. J.E. Truman, M.J. Coleman, and K.R. Pirt, *Br. Corros. J.*, Vol 12, 1977, p 236
22. R.C. Newman, Y.C. Lu, R. Bandy, and C.R. Clayton, *Proceedings of the Ninth International Congress on Metallic Corrosion*, National Research Council, Toronto, Vol 1, 1984, p 394
23. C.R. Clayton, *Passivity Mechanisms in Stainless Steels: Mo-N Synergism*, Report No. N00014-85-K-0437, State University of New York at Stony Brook, Stony Brook, New York, 1986
24. U. Kamachi Mudali, R.K. Dayal, T.P.S. Gill, and J.B. Gnanamoorthy, *Werkst. Korros.*, Vol 37, 1986, p 637
25. U. Kamachi Mudali, R.K. Dayal, T.P.S. Gill, and J.B. Gnanamoorthy, *Corrosion*, Vol 32, 1990, p 454
26. U. Kamachi Mudali, R.K. Dayal, J.B. Gnanamoorthy, and P. Rodriguez, Pitting Corrosion and Passive Film Stability of Nitrogen Bearing Austenitic Stainless Steels, 42nd Annual Technical Meeting of The Indian Institute of Metals, November 14-17, 1988
27. C.R. Clayton and K.G. Martin, *Proceedings of the International Conference on High Nitrogen Steels HNS 88*, The Institute of Metals, Lille, France, 1988, p 256
28. A.J. Sedriks, *Corrosion of Stainless*, John Wiley & Sons, 1979, p 63
29. R.C. Newman and T. Shahrabi, *Corros. Sci.*, Vol 27, 8; 1987, p 827
30. P.G. Laing, Biocompatibility of Biomaterials, *Orthopaedic Clinics of North America*, C.M. Evarts, Ed., Vol 4, 1973, p 249